

# Computational Analysis of Thermal Behavior within a Scraped Surface Heat Exchanger (SSHE)

Rajesh S C, Gautham Krishnan, Sreehari P, Akhil Naryanan K, Sibin S Nair

Department of Mechanical Engineering, Mangalore Institute of Technology and Engineering,  
Moodabidri, Mangalore, Karnataka, India

**How to cite this paper:** Rajesh S C | Gautham Krishnan | Sreehari P | Akhil Naryanan K | Sibin S Nair "Computational Analysis of Thermal Behavior within a Scraped Surface Heat Exchanger (SSHE)" Published in International Journal of Trend in Scientific Research and Development (ijtsrd), ISSN: 2456-6470, Volume-3 | Issue-5, August 2019, pp.204-212, <https://doi.org/10.31142/ijtsrd25241>



IJTSRD25241

Copyright © 2019 by author(s) and International Journal of Trend in Scientific Research and Development Journal. This is an Open Access article distributed under the terms of the Creative Commons Attribution License (CC BY 4.0) (<http://creativecommons.org/licenses/by/4.0>)



## ABSTRACT

In this present work, the Computational analysis of fluid flow and heat transfer within a Scraped Surface Heat Exchanger (SSHE), which is an industrial device, is reported. The 3D model of SSHE geometry is achieved with Solid Edge V18. 3D mesh model of SSHE with finite volume discretization obtained in ANSYS ICM CFD code and ANSYS CFX V15 used to solve continuity, momentum and energy equations using multiple rotating reference frame formulation. The steady, laminar, non-isothermal flow of pure glycerin Newtonian fluid was investigated. The cooling process without phase change within the SSHE was studied. The different scraper blades of 3 and 2. The inlet velocity of the fluid is varied to evaluate the thermal behavior of SSHE. The different process parameters in the parametric study are rotational velocity, axial velocity and the different scraper blades (3 and 2). When reducing the number of rotating parts, better cooling is achieved. The variations of the local heat transfer coefficient based on inner wall temperature and bulk fluid temperature as a function of the main process parameters, namely rotational velocity, axial velocity and the different scraper blades obtained. The results have shown that viscous dissipation has a significant effect on the cooling of the glycerine. The local heat transfer coefficient increases gradually when reducing the rotating parts of scraper blades improves the heat transfer rate. Larger increases of the same occurred with higher rotational velocity and axial velocity. If higher the value of rotating velocity=9rps is considered there is a viscous heating occurs and also more number of rotating parts friction is produced on the boundary layer surface and the temperature increases, so 2 scraper blades results shows the better heat transfer performance in bulk fluid temperature and local heat transfer co-efficient. This is expected to be useful in the design of SSHEs handling highly viscous fluids.

**KEYWORDS:** Scraped Surface Heat Exchangers, Newtonian Fluid, Heat transfer co-efficient, bulk fluid temperature

## 1. INTRODUCTION

Scraped surface heat exchangers (SSHE) are used to prevent the deposition of substantial solids on the heat transfer surface. The construction consists of a double pipe with the process fluid in the inner pipe and acting and cooling or heating medium in the annulus. The inner wall of the tube is scraped with a rotating element which is equipped with a spring. There is an annular gap with cylindrical rotor and stator. Blades are provided which are in turn driven by the rotor.

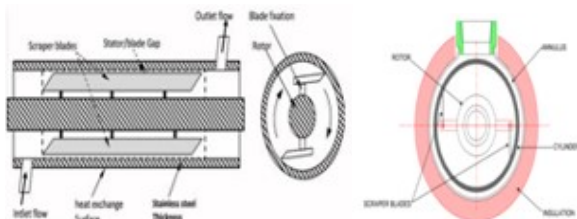


**Fig. 1.1 Schematic Representation of a SSHE, Longitudinal and Transversal Cross Section**

Scraping enhances the heat transfer by breaking the thermal and hydrodynamic boundary layers. Scraped Surface Heat Exchanger has capacity to thermally treat high viscous fluids. It has many applications in pharmaceutical, food, and chemical industries etc. It can be used for freezing, sterilization, gelatinization and cooling of the products. Fluids with high viscosity such as peanut butter, cream cheese, and mayonnaise etc. can be sterilized using SSHE. MounirBaccar et.al [1] performed a 3-D numerical simulation of the scraped surface heat exchanger with helical screw., the increase of the number of turns in the screws allows to increase the thermal efficiency of the SSHE. S. Ali, M.Baccar et. Al [3] performed a numerical 3D CFD analysis of heat transfer in a scraped surface heat exchanger for Bingham Fluids. The numerical results indicate that by increasing the Reynolds rotation, the Reynolds axial and Oldroyd numbers can improve the heat transfer. TiborVarga et.al[4] conducted a study on the flow characteristics and pressure drop within the horizontal scraped surface heat exchanger the use of different types of mixers does not have a significant effect on the speed profile, when the product is

already managed by rotary scrapers. Whereas, it has a quite significant impact on the pressure drop, which can lead to a higher energy consumption. Denis Flick [5] et.al modeled the flow and heat transfer in a scraped surface heat exchanger during sorbet production, the occurrence of recirculation near the blade endings allows back flow from the outlet region. Parikh [6] et.al performed a thermal analysis of the scraped surface heat exchanger used in the food industries. The milk is used as working fluid and water to cool the medium, CFD analysis shows that milk cooling increases using a small scraper design than the full blade design. S. Ali et.al [8] conducted an experimental study on the performance of the surface heat exchanger scraped with helical tapes, found that when the number of turns increases, the heat transfer increases and the phenomenon of the reverse mix is close to disappearing.

**A. PRINCIPLE OF SSHE**

A typical SSHE consist of two cylinders, a heated or cooled outer cylinder and a rotating inner cylinder. The fluid flows along the annulus between these two. The inner cylinder is attached with blades scrap the outer cylinder surface periodically to prevent film formation. They also promote mixing and heat transfer. The tip of the blades forms a high shear region. The significant thermal effects due to viscous dissipation in this region makes it necessary to understand the local shear and the thermal effects in order to predict the heat transfer performance.

**B. OBJECTIVE**

- Comparing the two blade, three blade designs of scraped surface heat exchanger and analyzing the blades effect on heat transfer rate.
- The steady state laminar non-isothermal flow of pure glycerin (Newtonian fluid) of temperature dependent viscosity of fluid is investigated.
- Analyzing the bulk fluid temperature at different cross section of heat exchanger.
- Analyzing the heat transfer coefficient at different cross section of heat exchanger.
- Analyzing the effect of rotational speed on heat transfer rate.

**2. DESIGN CONSIDERATIONS AND FLUID PROPERTY**

3D model (three dimensional) representing real industrial scraped surface heat exchanger geometry has been modeled using solid edge software.

Two models of the scraped surface heat exchanger has been built.

- Scraped surface heat exchanger having two blades.
- Scraped surface heat exchanger having three blades.

In view of the geometry, the Cartesian coordinate system is chosen to describe the geometry, where x, y and z axes are took in the horizontal, vertical and axial direction of SSHE respectively.

**A. DESIGN PARAMETERS**

TABLE2.1. DESIGN PARAMETERS OF SSHE

PARAMETERS	CHARACTERISTICS
Stator Diameter $D_s$	0.065 m
Rotor Diameter $D_r$	0.04 m
Stator Length L	0.4 m
Total Surface Area of Heat Exchanger $S_{ex}$	0.0883 m <sup>2</sup>
Total Volume $V_t$	0.00132 m <sup>3</sup>
Blade-Stator Clearance	130 $\mu$ m
Number of Blades	2, 3

TABLE2.2. MATERIALS USED IN SSHE

PART	MATERIAL
Blade	Stainless Steel 410
Rotor	Stainless Steel 316L
Stator	Stainless Steel 316L

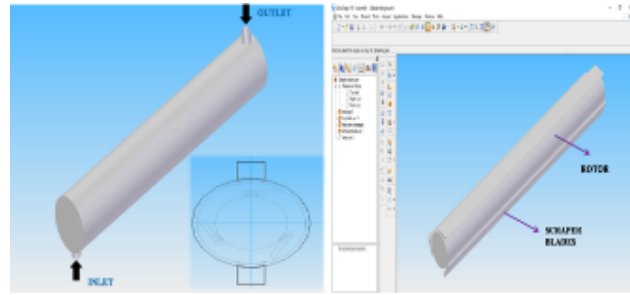


Fig. 2.2 Stator

Fig. 2.3 3Blade Design of SSHE

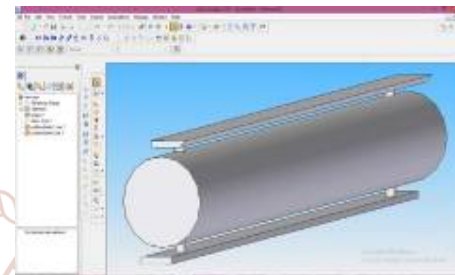


Fig 2.4 Two Blade Design of SSHE

**B. FLUID PROPERTY**

- Molar mass of pure glycerin : 0.092 kg/mol
- Density : 1240 kg/m<sup>3</sup>
- Specific heat capacity: 2435 J/kg k
- Dynamic viscosity : 1.4 pas sec
- Thermal conductivity : 0.285 W/m k

**3. MESHING**

The process of meshing is used here is a tetrahedral meshing which is carried out in two designs named as 2 blade and 3 blade respectively .High quality mesh is selected from the grid independent study.

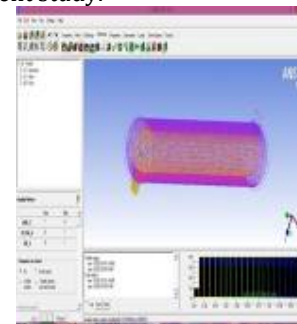


Fig 3.3 Meshed Two Blade SSHE

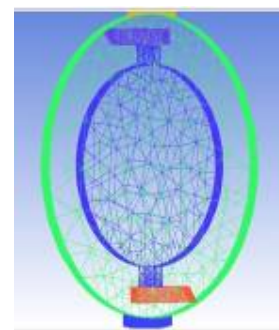


Fig 3.4 Cross Sectional View of Two blades SSHE

#### 4. GRID INDEPENDENT STUDY

Grid independency is a very important issue in numerical simulation to find out the optimum mesh value. Grid independent means calculation results changes so little along with a denser or looser grid that the truncation error can be ignored in numerical simulation. When considering grid independent issue, in principle a very dense grid can avoid this problem but the calculation resource maybe wasted unnecessarily. In practice, we usually increase the grid resolution according to certain interval spacing, and then compare the results of two neighborhood results. If the results tend towards identical, the grid can be considered as grid independent. Such strategy and that ratio can be used for the generation of further grids.

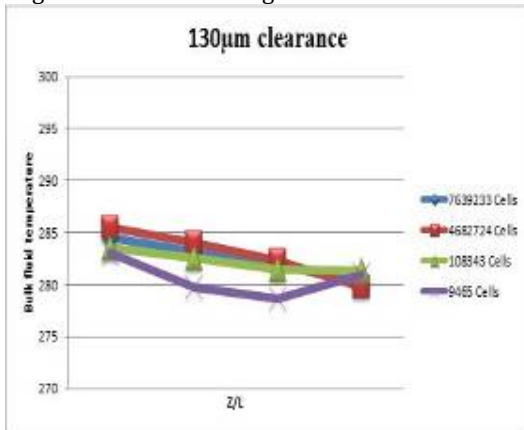


Fig 4.1 Grid independence Study of Three Blade SSHE

Good quality tetrahedral grids can be generated through a commercially available meshing tool. A structural mesh superimposed with ICEM CFD software meshing tool (version 14.5). The density of the mesh increases near the wall and especially in the clearance region to ensure accuracy there, as higher temperature changes in the fluid are expected to occur in these regions. There are at least 4 mesh points across the tip of the clearance and the mesh turned out to be highly concentrated at the tip of the blades. This was done by performing a series of simulations with different mesh sizes, starting from a cores mesh and refining it until the physical results were no longer dependent on the size of the mesh. Good discretization accuracy were retained through tetrahedral cells. Four mesh refinements of 7639233, 4682724, 108343 and 9465 cells were tested and compared with a physical parameter of the bulk fluid temperature for each cross-section of SSHE as shown in fig.4.1. For good accuracy of results a fine mesh of 7639233 cells is chosen for further analysis.

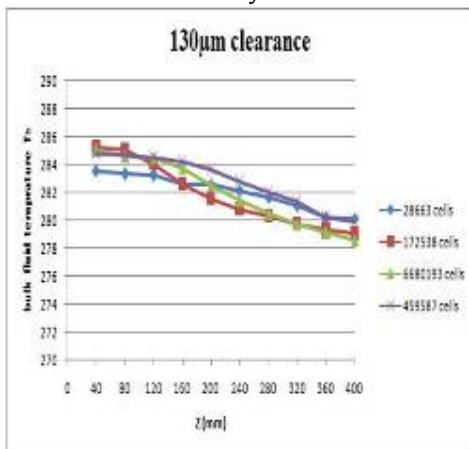


Fig 4.2 Grid Independent Study of Two Blade SSHE

This was done by performing a series of simulations with different mesh sizes, starting from a cores mesh and refining it until the physical results were no longer dependent on the size of the mesh. Good discretization accuracy was retained through tetrahedral cells. Four mesh refinements of 28663, 172538, 459587 and 6680193 cells were tested and compared with a physical parameter of the bulk fluid temperature for each cross-section of SSHE as shown in fig.4.1. For good accuracy of results a fine mesh of 6680193 cells is chosen for further analysis.

#### 5. PHYSICAL PROBLEM DISCRIPTION

A scraped surface heat exchanger is generally used to cool or heat viscous fluids with high viscosity. The flow of fluids and the heat transfer in SSHE is complex and has not been understood up to this point. Figure 1.5 shows a schematic representation of an SSHE; two blades and three blades were considered in this study. The operating principle of SSHE is as follows:

The heated or cooled fluid enters the exchanger through a flange (flow inlet), and mixed with blades (sheared zone), and exits through another flange (flow outlet) (Fig.1.5). During this operation, the treated fluid is contacted with a heat transfer surface (stator wall) that is scraped quickly and continuously, thus exposing the surface to the passage of the untreated fluid. Along with maintaining a good and uniform heat exchange, the scraper blades also provide simultaneous mixing and agitation. Heat exchange for sticky, viscous foods, such as a heavy salad dressings, margarine, chocolate, peanut butter, fondant, ice cream, and shortening is possible only through the use of SSHEs. High heat transfer coefficients are achieved because the boundary layer is continuously replaced by fresh material. The enhancement of the thermal efficiency must be guaranteed by the scraping action of the blades. The dimensions of the simulated SSHE are summarized in Table 2.1. This document was intended to shed new light on heat transfer behavior by numerical resolution of continuity, momentum and energy equations within a scraped surface heat exchanger. A 3D-numerical model that represents the geometry of the actual industrial heat exchanger has achieved and coupled using the SOLID EDGE and ANSYS ICEM CFD tool. First, the possible thermal correlations in the literature were compared with the results of current numerical calculations, based on the determinations of the average convective heat coefficient. Temperature difference between the entrance and the cooled wall was taken equal to 10 K. This situation is usually found for the cooling process in SSHE, in which the fluid enters SSHE at a temperature of 288 K (15°C) and it is cooled to the temperature of 278 K (5°C).

#### 6. GOVERNING EQUATIONS AND NUMERICAL DETAILS

This section lists the governing equations for heat transfer and fluid flow, including viscous dissipation in the SSHE. They have considered steady state, not isothermal, incompressible. It is assumed that the flow is laminar throughout the computation. Reynolds number of rotation is less than 50 and axial Reynolds number less than 2.

The equations for continuity, momentum and energy for the incompressible flows have been resolved in dimensional form. It is pertinent to use rotation formulation of the frame of reference to solve the equations of continuity, momentum and energy. The main reason for using the movement frame of reference is to address a problem that is unstable in the

steady frame (inertial) constant with respect to the frame in motion. Here we are neglecting the effects of gravity; however, it is easy to include it in the axial pressure gradient if SSHE mounts with the vertical axis. The wall of the stator (heat exchange surface) was taken into account with a thickness of 5 mm.

It is pertinent to use the Steady state rotating reference frame formulation to solve Continuity, Momentum & Energy Equations with a dimensionless as follows:

**A. CONTINUITY EQUATION**

$$u \frac{\partial u}{\partial x} + v \frac{\partial v}{\partial y} + w \frac{\partial w}{\partial z} = 0$$

**B. MOMENTUM EQUATION**

➤ X DIRECTION

$$\left( u \frac{\partial u}{\partial x} + v \frac{\partial u}{\partial y} + w \frac{\partial u}{\partial z} \right) + \left( 2\omega v_r \right) + \left( \omega^2 r \right) = - \frac{\partial p}{\partial x} + \mu \left( \frac{\partial^2 u}{\partial x^2} + \frac{\partial^2 u}{\partial y^2} + \frac{\partial^2 u}{\partial z^2} \right)$$

Where,

$(2\omega \times v_r)$  Is the Coriolis acceleration

$(\omega^2 \times r)$  Is the Centripetal acceleration

➤ Y DIRECTION

$$\left( u \frac{\partial v}{\partial x} + v \frac{\partial v}{\partial y} + w \frac{\partial v}{\partial z} \right) + \left( 2\omega v_r \right) + \left( \omega^2 r \right) = - \frac{\partial p}{\partial y} + \mu \left( \frac{\partial^2 v}{\partial x^2} + \frac{\partial^2 v}{\partial y^2} + \frac{\partial^2 v}{\partial z^2} \right)$$

➤ Z DIRECTION

$$\left( u \frac{\partial w}{\partial x} + v \frac{\partial w}{\partial y} + w \frac{\partial w}{\partial z} \right) + \left( 2\omega v_r \right) + \left( \omega^2 r \right) = - \frac{\partial p}{\partial z} + \mu \left( \frac{\partial^2 w}{\partial x^2} + \frac{\partial^2 w}{\partial y^2} + \frac{\partial^2 w}{\partial z^2} \right)$$

**C. ENERGY EQUATION**

$$\underbrace{\left( u \frac{\partial T}{\partial x} + v \frac{\partial T}{\partial y} + w \frac{\partial T}{\partial z} \right)}_{\text{Forced heat convection}} = k \underbrace{\left( \frac{\partial^2 T}{\partial x^2} + \frac{\partial^2 T}{\partial y^2} + \frac{\partial^2 T}{\partial z^2} \right)}_{\text{Conduction}} + \underbrace{\phi}_{\text{Viscous heating}}$$

$$\phi = \mu \left\{ 2 \left[ \left( \frac{\partial u}{\partial x} \right)^2 + \left( \frac{\partial v}{\partial y} \right)^2 + \left( \frac{\partial w}{\partial z} \right)^2 \right] + \left( \frac{\partial v}{\partial x} + \frac{\partial u}{\partial y} \right)^2 + \left( \frac{\partial w}{\partial y} + \frac{\partial v}{\partial z} \right)^2 + \left( \frac{\partial u}{\partial z} + \frac{\partial w}{\partial x} \right)^2 \right\}$$

**D. ENERGY EQUATION FOR SOLID STEADY STATE HEAT CONDUCTION**

$$\rho C_p \left[ u \frac{\partial T}{\partial x} + v \frac{\partial T}{\partial y} + w \frac{\partial T}{\partial z} \right] = k \left( \frac{\partial^2 T}{\partial x^2} + \frac{\partial^2 T}{\partial y^2} + \frac{\partial^2 T}{\partial z^2} \right)$$

**7. BOUNDARY CONDITIONS**

In this work we have analyzed the fluid cooling process occurring in an SSHE. For the fluid flow, the momentum equation, boundary conditions are given as follows: The fluid (glycerin) is introduced at the inlet with the temperature of T-inlet=288K, and was cooled with the constant outer wall temperature Tw=278K. The temperature difference between the wall heat exchanger and fluid inlet was ΔT=10K. Adiabatic conditions were assumed for the rotor and scraper blade. Zero temperature gradient is assumed at the outlet.

ANSYS CFX code uses the finite volume method for discretization. A segregated approach can be solved with governing steady state equations for mass and momentum conservation. Here, the equations are sequentially solved with implicit linearization. A second-order upwind were approximated using Volume-faces advective fluxes interpolation scheme. A coupling between velocity and temperature fields must be considered because of the effect of the viscosity variation due to heat transfer. The pressure-velocity coupling is implemented using iterative correction procedure (SIMPLEC algorithm). For the energy equation too, a second-order upwind interpolation scheme is used.

- Inlet temperature of the fluid = 288 K
- $V = V_{axial} = \frac{Q}{A}$
- Q= Volume flow rate (m<sup>3</sup>/s)
- A= Area of the fluid region
- r = Radius of the fluid region
- Rotating velocity(ω) = 3, 6 and 9 rps
- Cooling temperature of the surface = 278 K
- Axial Reynolds Number =  $\frac{\rho V D}{\mu}$
- Rotational Reynolds Number =  $\frac{\rho \omega D^2}{\mu}$
- ρ = Density of glycerin = 1240kg/m<sup>3</sup> at 15°C
- V = Velocity of the fluid (m/s)
- D= Diameter of the fluid region
- μ = Dynamic viscosity of the fluid = 1.4 Pa sec

TABLE 7.1 BOUNDARY CONDITIONS

Volume Flow Rate, Q m <sup>3</sup> /s	Axial Velocity, V <sub>axial</sub> m/s	Rotational Velocity/angular velocity, ω rps	Axial Reynolds Number, Re <sub>axial</sub>	Rotational Reynolds Number, Re <sub>rotational</sub>
2.77*10 <sup>-5</sup>	0.009796	3	0.52058	159.43
4.16*10 <sup>-5</sup>	0.0147	6	0.7812	318.86
5.55*10 <sup>-5</sup>	0.0196	9	1.0416	478.29

## 8. CODE VALIDATION

ANSYS CFX CFD code is used to solve the problem. The results of Yataghene [9] are reproduced in order to check for the accuracy and correctness of the code. It deals with the CFD analysis for various rotational velocities with a constant volumetric flow rate. Heat transfer coefficient is calculated for pure glycerin by varying rotational velocities in the range 3-10 rev/s. Fig. 4 shows the comparison of the results of Yataghene [9] and the present ICFM CFD results. From this we can come to a conclusion that the variations are almost identical except that the present results show slightly higher values. This level of agreement is considered satisfactory. It should be remembered that when increasing the rotational velocities, the temperature increases due to viscous dissipation of the fluid. Also, it may be noted that the increase in the rotational velocity increases the heat transfer coefficient of the fluid. The difference in the value obtained while comparing our present work and Yataghene's work is 11.9%.

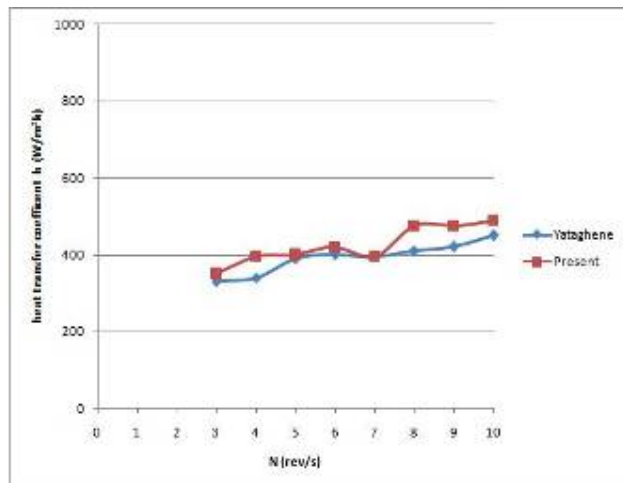


Fig 8.1 Code Validation

## 9. RESULT AND DISCUSSION

In order to obtain the performance characteristics of 3D model of SSHE for the fluid flow and heat transfer, a parametric study is carried out by varying number of scraper blades 2 and 3, by keeping tip clearance between blade and stator wall as 130  $\mu\text{m}$ , the rotational velocity of the rotor and the axial velocity of the fluid entering the SSHE. The rotational velocity of blades are provided with 3, 6, 9 rps and axial velocity of fluid entering the inlet is given as 0.009796, 0.0147, and 0.0196 m/s. Graphs are plotted to show the variation of bulk fluid temperature along the length of scraped surface heat exchanger. Another graph is plotted with variation of heat transfer coefficient along the length of SSHE. The local heat transfer coefficient is calculated with the equation given below with respect to the axial distance.

$$h = q_w / (T_{\text{bulk}} - T_{\text{wall}}) \quad (9.1)$$

Where,  $Q = mc_p \Delta T$

$Q$  is the heat transfer

$m$  is mass flow rate (kg/sec)

$A$  is total surface area of the stator ( $\text{m}^2$ )

$C_p$  is the specific heat

$\Delta T$  Is the temperature difference of the fluid between inlet and outlet

$T_{\text{bulk}}$  is the bulk fluid temperature (K)

$T_{\text{wall}}$  is the stator wall temperature (K)

Where  $q_w = Q/A$  is heat flux

The local heat transfer coefficient based on the temperature of the internal wall and the temperature of the bulk fluid was calculated by using the above equation along the axial distance of SSHE. The general variation of the local heat transfer coefficient reveals that it is of high value near the inlet section of the exchanger because the thickness of the boundary layer is very small. It decreases continuously due to the increase in the thickness of the thermal boundary layer. By increasing the number of scraper blades (ie, 4 and 3 compared to 2 scraper blades), a better local heat transfer coefficient is achieved and an improvement in SSHE performance is obtained by achieving a thermally developed fluid flow.

### A. AXIAL VARIATIONS OF BULK FLUID TEMPERATURE FOR 3BLADES

The Figs 8.1 to 8.3 shows the variation of the bulk fluid temperature versus the Z-coordinate (or the axial distance of SSHE). Fig 8.10 pertains to  $\omega=3\text{rps}$  and varying axial velocity of, namely,  $V_{\text{axial}}=0.09796, 0.0147$  and  $0.0196\text{m/s}$ . For  $v=0.6$ , the inner wall temperature and the bulk fluid temperature is higher at the entrance region, because of the thickness of the boundary layer is very small at the inlet section. When comparing the two curves of the bulk fluid temperature at different axial velocity, it can be seen that these two curves are almost parallel to each other and we can say that the temperature difference is uniformly distributed to the fluid along the axial distance of the SSHE with the low axial velocity of the fluid and better cooling of the fluid takes place.

The Figs 8.2 and 8.3 shows that when increasing the rotational velocity to higher values, i.e., when the rotational velocity is progressively chosen as  $\omega=6\text{rps}$  and  $9\text{rps}$ , the bulk fluid temperature gradually decreases with increasing values of axial velocity and rotational velocity. The inner wall temperature increases because of the thickness of the boundary layer increases with higher values of axial velocity of the fluid. This results in lower thermal resistance between the bulk of the fluid and the inner wall. The bulk fluid temperature decreases at the exit section ( $Z=400\text{mm}$ ) with increasing values of rotational velocity. Whether the bulk fluid temperature increases or decreases depends upon three opposing factors, namely, the cooling at the wall, the viscous dissipation and more number of rotating parts. In the case of 3 scraper blades

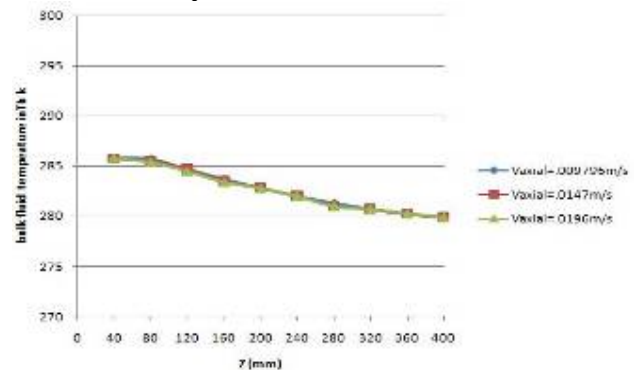
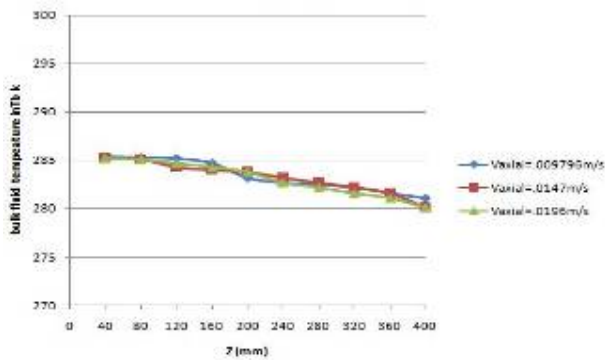
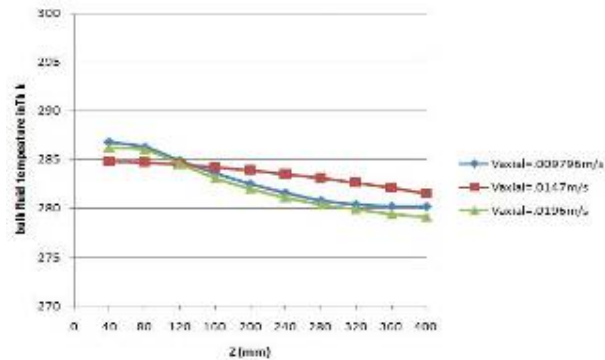


Fig 8.1 Axial Variation of Bulk Fluid Temperature at  $\omega=3\text{rps}$  and varying axial velocity,  $V_{\text{axial}}=0.09796, 0.0147$  and  $0.0196\text{m/s}$



**Fig 8.2 Axial Variation of Bulk Fluid Temperature at  $\omega=6$ rps and varying axial velocity,  $V_{axial}=0.09796$ , 0.0147 and 0.0196m/s**



**Fig 8.3 Axial Variation of Bulk Fluid Temperature at  $\omega=9$ rps and varying axial velocity,  $V_{axial}=0.09796$ , 0.0147 and 0.0196m/s**

**B. AXIAL VARIATIONS OF LOCAL HEAT TRANSFER COEFFICIENT BASED ON BULK FLUID TEMPERATURE FOR 3 BLADE DESIGN**

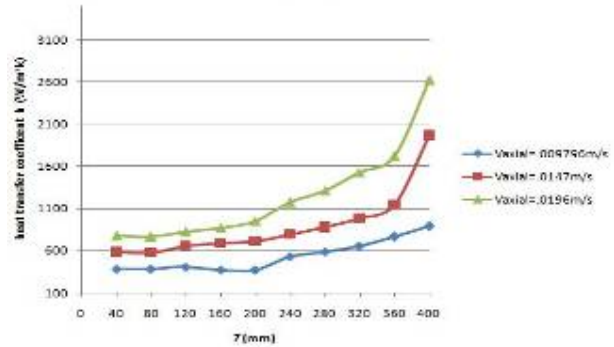
The Fig 8.3 to 8.6, show the distribution of the local heat transfer coefficient. These figures are plots of wall temperature and bulk fluid temperature V/s Z-axial distance of SSHE. The local heat transfer coefficient is calculated based on Eq. (8.1) at each cross-section of the SSHE.

Fig 8.3 shows the results for  $\omega=3$ rps and varying axial velocity, namely,  $V_{axial}=0.009796$ , 0.0147 and 0.0196 m/s. For  $V_{axial}=0.009796$  we observe the general variation of local heat transfer coefficient reveals that it is of lower value near the entrance region of the exchanger because the thickness of the thermal boundary layer is too large. It increases continuously due to decrease the thermal boundary layer thickness and produces a thermally fully developed flow. The thermal development is achieved within the total axial distance chosen for the SSHE.

For  $V_{axial}=0.0147$  and 0.0196 m/s, the local heat transfer coefficient slightly increases. This is because, with the axial distance, the heat flux increases and temperature difference between the inner wall and the bulk fluid decreases. The thermal boundary layer increases with increasing axial velocity and produces thermally fully developed flow within the chosen length of the SSHE.

The Figs 8.4 to 8.6, show that for increasing values of rotational velocity i.e. for  $\omega=6$  and 9rps, the local heat transfer coefficient increases. The same thing also happens with higher values of axial velocity. The temperature difference (between the inner wall and the bulk fluid) decreases with higher values of the axial velocity. It can also be seen that thermally fully developed flow is achieved in the SSHE. The local heat transfer coefficient for 3 scraper blades

is very low compared to 2 scraper blades, because if it contains more number of rotating parts the fluid doesn't mix properly and also viscous heating occurs between the surface and the tip of the blades.



**Fig 8.4 Axial Variations of Local Heat Transfer at  $\omega=3$ rps and varying axial velocity,  $V_{axial}=0.09796$ , 0.0147 and 0.0196m/s**

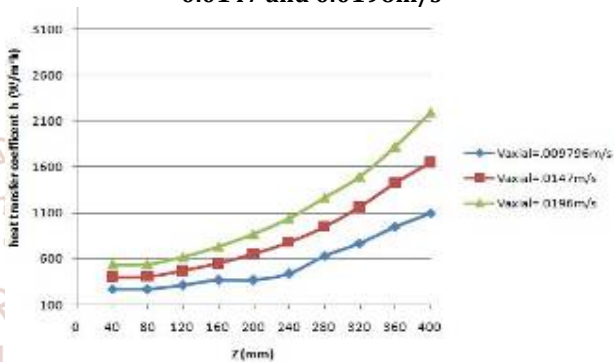


**Fig 8.5 Axial Variations of Local Heat Transfer Coefficient at  $\omega=6$ rps and varying axial velocity,  $V_{axial}=0.09796$ , 0.0147 and 0.0196m/s**

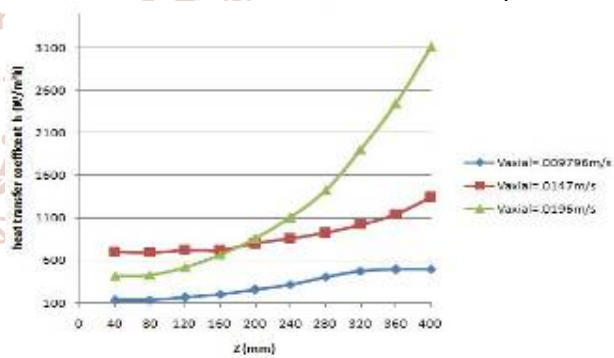


**Fig 8.6 Axial Variations of Local Heat Transfer Coefficient at  $\omega=9$ rps and varying axial velocity,  $V_{axial}=0.09796$ , 0.0147 and 0.0196m/s**

**C. AXIAL VARIATIONS OF BULK FLUID TEMPERATURE FOR 2BLADE DESIGN**

The Figs 8.7 to 8.9 shows the variation of the bulk fluid temperature versus the Z-coordinate (or the axial distance of SSHE). Fig 1 (a) pertains to  $\omega=3$ rps and varying axial velocity of, namely,  $V_{axial}=0.09796$ , 0.0147 and 0.0196m/s. For  $v=0.6$ , the inner wall temperature and the bulk fluid temperature is higher at the entrance region, because of the thickness of the boundary layer is very small at the inlet section. When comparing the two curves of the bulk fluid temperature at different axial velocity, it can be seen that these two curves are almost parallel to each other and we can say that the temperature difference is uniformly distributed to the fluid along the axial distance of the SSHE with the low axial velocity of the fluid and better cooling of the fluid takes place.

The Figs 8.8 and 8.9 shows that when increasing the rotational velocity to higher values, i.e., when the rotational velocity is progressively chosen as  $\omega=6$ rps and 9rps, the bulk fluid temperature gradually decreases with increasing values of axial velocity and rotational velocity. The inner wall temperature increases because of the thickness of the boundary layer increases with higher values of axial velocity of the fluid. This results in lower thermal resistance between the bulk of the fluid and the inner wall. The bulk fluid temperature decreases at the exit section ( $Z=400$ mm) with increasing values of rotational velocity. This graph shows that reducing the number of rotating parts better cooling process occurs at the exit section.

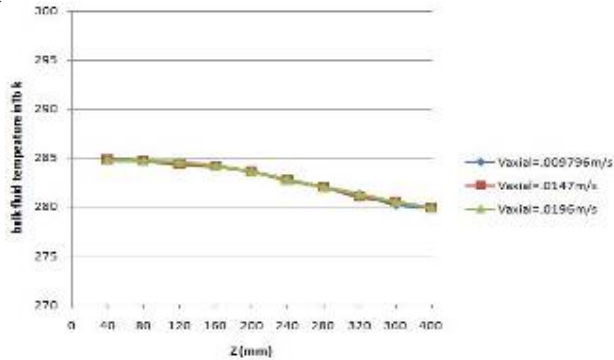


**Fig 8.7 Axial Variation of Bulk Fluid Temperature at  $\omega=3$ rps and varying axial velocity,  $V_{axial}=0.09796, 0.0147$  and  $0.0196$ m/s**

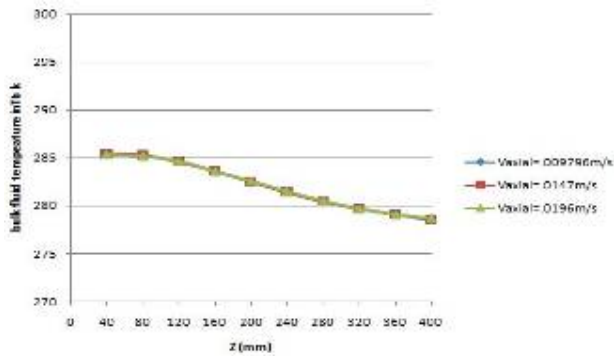


**Fig 8.8 Axial Variation of Bulk Fluid Temperature at  $\omega=6$ rps and varying axial velocity,  $V_{axial}=0.09796, 0.0147$  and  $0.0196$ m/s**

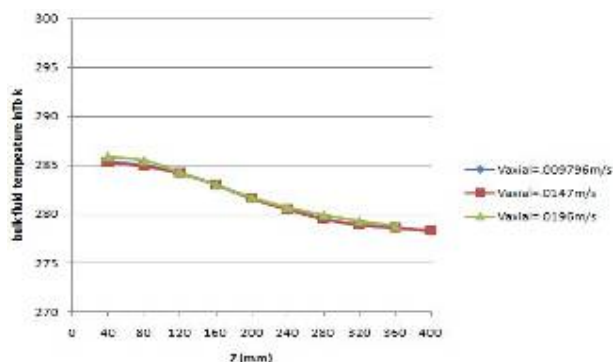


**Fig 8.9 Axial Variation of Bulk Fluid Temperature at  $\omega=9$ rps and varying axial velocity,  $V_{axial}=0.09796, 0.0147$  and  $0.0196$ m/s**

**D. AXIAL VARIATIONS OF LOCAL HEAT TRANSFER COEFFICIENT BASED ON BULK FLUID TEMPERATURE FOR 2 BLADE DESIGN**

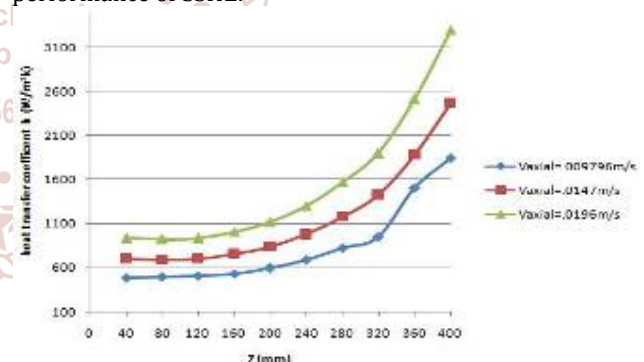
The Fig 8.10 to 8.12, show the distribution of the local heat transfer coefficient. These figures are plots of wall

temperature and bulk fluid temperature V/s Z-axial distance of SSHE. The local heat transfer coefficient is calculated based on Eq. (7.1) at each cross-section of the SSHE.

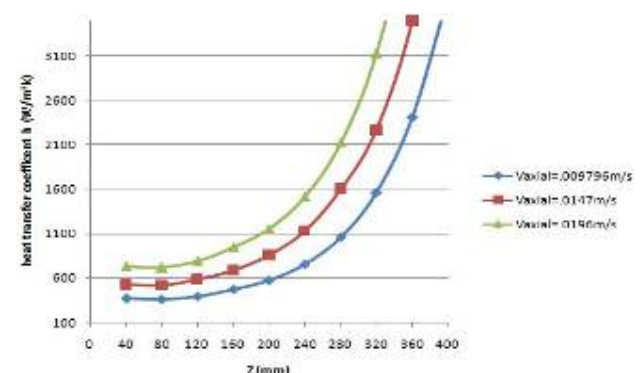
Fig 8.10 shows the results for  $\omega=3$ rps and varying axial velocity, namely,  $V_{axial}=0.009796, 0.0147$  and  $0.0196$  m/s. For  $V_{axial}=0.009796$  we observe the general variation of local heat transfer coefficient reveals that it is of lower value near the entrance region of the exchanger because the thickness of the thermal boundary layer is too large. It increases continuously due to decrease the thermal boundary layer thickness and produces a thermally fully developed flow. The thermal development is achieved within the total axial distance chosen for the SSHE.

For  $V_{axial}= 0.0147$  and  $0.0196$  m/s, the local heat transfer coefficient slightly increases. This is because, with the axial distance, the heat flux increases and temperature difference between the inner wall and the bulk fluid decreases. The thermal boundary layer increases with increasing axial velocity and produces thermally fully developed flow within the chosen length of the SSHE.

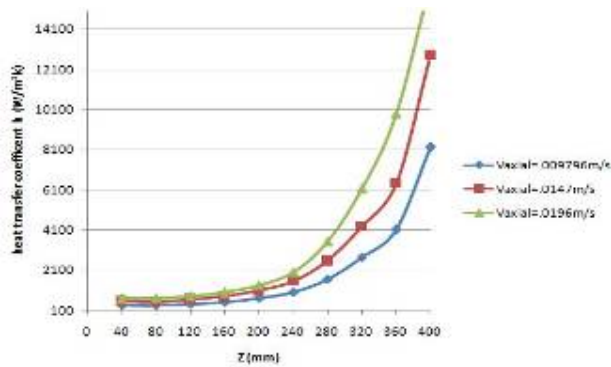
The Figs 8.11to 8.12, show that for increasing values of rotational velocity i.e. for  $\omega=6$  and 9rps, the local heat transfer coefficient increases. The same thing also happens with higher values of axial velocity. The temperature difference (between the inner wall and the bulk fluid) decreases with higher values of the axial velocity. It can also be seen that thermally fully developed flow is achieved in the SSHE. The local heat transfer coefficient is very high compared to 3 scraper blades, because the local heat transfer coefficient increases with reducing number of rotating parts and it scrape the boundary layer and improve the performance of SSHE.



**Fig 8.10 Axial Variations of Local Heat Transfer Coefficient at  $\omega=3$ rps and varying axial velocity,  $V_{axial}=0.09796, 0.0147$  and  $0.0196$ m/s**



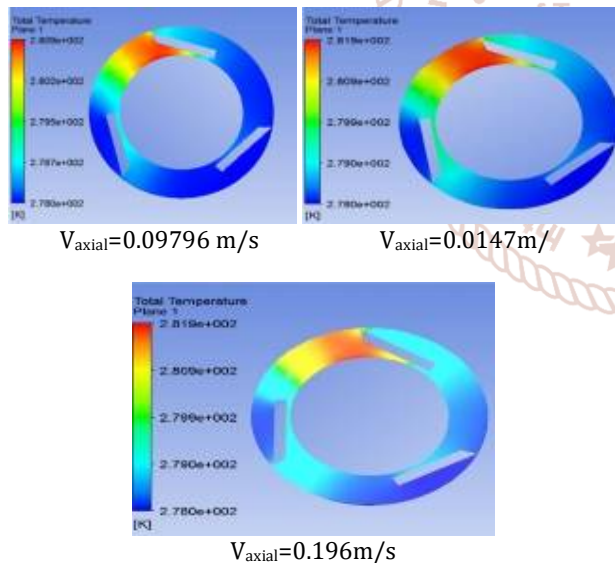
**Fig 8.11 Axial Variations of Local Heat Transfer Coefficient at  $\omega=6$ rps and varying axial velocity,  $V_{axial}=0.09796, 0.0147$  and  $0.0196$ m/s**



**Fig8.12 Axial Variations of Local Heat Transfer Coefficient at  $\omega=9\text{rps}$  and varying axial velocity,  $V_{axial}=0.09796, 0.0147$  and  $0.0196\text{m/s}$**

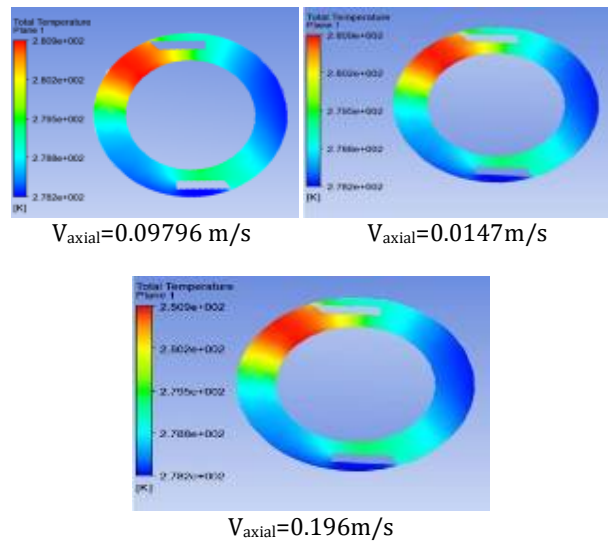
**E. E. AXIAL VARIATION OF BULK FLUID TEMPERATURE OF 3 and 2 blades.**

Fig. 8.13 temperature contours can be seen that, the temperature decreases at the different cross-section of Z between the rotor wall and the tip of the blade as the angular velocity increases. This shows better cooling is take place with the increase in the angular velocity scraping the boundary layer and transfer the wall temperature to the inner fluid to achieve the cooling process. As a matter of fact, more number of rotating parts contains better cooling should takes place but in the 3 scraper blades it is achieving higher temperature because the rubbing action that takes place in the fluid between the blade and the stator wall causes viscous dissipation, which oversees the cooling process caused due to the wall at lower temperature.



**Fig. 8.13 Temperature distribution at the outlet for 3 blade design when the outlet when  $\omega = 3\text{rps}$  for different axial velocity,  $V_{axial}=0.09796, 0.0147$  and  $0.0196\text{m/s}$**

Fig 8.14 temperature contours can be seen that the temperature decreases at the different cross-section of Z between the rotor wall and the tip of the blade as the angular velocity increases. This shows better cooling is take place with the increase in the angular velocity scraping the boundary layer and transfer the wall temperature to the inner fluid to achieve the better cooling process compare to 3 scraper blades.



**Fig. 8.14 Temperature distribution at the outlet for 2 blade design when the outlet when  $\omega = 3\text{rps}$  for different axial velocity,  $V_{axial}=0.09796, 0.0147$  and  $0.0196\text{m/s}$**

**10. CONCLUSIONS**

The 3D numerical model is employed to examine the thermal performance of an industrial scraped surface heat exchanger device. The geometry mesh is generated with tetrahedral cells for better discretization of momentum and energy equations. Pure glycerin, treated as a Newtonian fluid is examined with main process parameters of axial velocity, rotational velocity and different scraper blades. The local heat transfer coefficient based on surface wall temperature and bulk fluid temperature is numerically computed for several operating conditions of the SSHE with respect to axial distance. A parametric study is done and the following conclusions are reached.

The flow and temperature distributions produce better cooling or lower outlet temperature only when reducing the number of rotating parts (scraper blades) and there is a good heat removal at the boundary surface. This is confirmed by the results pertaining to the two scraper blades.

- The different cross section of axial distance (Z-axis) shows that higher the rotational velocity decreases the outlet temperature when reducing the number of rotating parts.
- The local heat transfer coefficient based on inner wall temperature and bulk fluid temperature increases along the length of the SSHE in the axial direction with decreasing the number of scraper blades.
- In case of 3 scraper blades, the local heat transfer coefficient is very less compared to 2 scraper blades because the number of scraper blade increases with higher values of rotational velocity viscous dissipation occurs and thereby heat transfer decreases. For 2 scraper blades scrape the boundary layer at the surface and this increases the local heat transfer coefficient.
- The local heat transfer coefficient increases with increasing rotational velocity; this improves the performance of the SSHE.

**REFERENCES**

[1] RabebTriki, HasseneDjemel, MounirBaccar “3-D NUMERICAL SIMULATION OF SCRAPPED SURFACE HEAT EXCHANGER WITH HELICAL SCREW”, World Academy of Science, Engineering and Technology

International Journal of Mechanical and Mechatronics Engineering Vol:12, No:6, 2018

- [2] Shicheng Li a\*, Chunsheng Zhou "HEAT TRANSFER ANALYSIS OF SCRAPED SURFACE HEAT EXCHANGER" International Conference on Material Science, Energy and Environmental Engineering (MSEEE 2017) Advances in Engineering Research, volume 125.
- [3] Ali S and Baccar M. "CFD ANALYSIS OF HEAT TRANSFER IN A SCRAPED SURFACE HEAT EXCHANGER FOR BINGHAM FLUID" 12th International Conference on Heat Transfer, Fluid Mechanics and Thermodynamics.
- [4] Tibor Varga, Gabor L. Szepesi, Zoltan Simenfalvi "FLOW CHARACTERISTIC AND PRESSURE DROP INSIDE THE HORIZONTAL SCRAPED SURFACE HEAT EXCHANGER" MultiScience - XXX. Micro CAD International Multidisciplinary Scientific Conference University of Miskolc, Hungary, 21-22 April 2016, ISBN 978-963358-113-1.
- [5] Oscar Dario- Hernandez Parra, Artemio Plana Fattori, Graciela Alvarez, Fatou-Toutie Ndoye, Hayat Benkhelifa, Denis Flick "MODELING FLOW AND HEAT TRANSFER IN A SCRAPED SURFACE HEAT EXCHANGER DURING THE PRODUCTION OF SORBET" Journal of food engineering, 2017 Elsevier Ltd.
- [6] Gandhi Nilay., Prexa Parikh "THERMAL ANALYSIS OF SCRAPED SURFACE HEAT EXCHANGER USED IN FOOD INDUSTRIES" IJSET - International Journal of Innovative Science, Engineering & Technology, Vol. 2 Issue 5, May 2015.
- [7] Frank G. F. Qin, Shashini Premathilaka, Xiao Dong Chen<sup>1</sup>, and Kevin W. Free "THE SHAFT TORQUE CHANGE IN A LABORATORY SCRAPED SURFACE HEAT EXCHANGER USED FOR MAKING ICE SLURRIES" Asia-Pac. J. Chem. Eng. 2007; 2:618630 Published online 13 September 2007 in Wiley InterScience.
- [8] Mourad Yataghene, Jack Legrand, "A 3D-CFD MODEL THERMAL ANALYSIS WITHIN A SCRAPED SURFACE HEAT EXCHANGER". Computers & Fluids, 71, 380-399 (2013).
- [9] S. Ali, M. Baccar "PERFORMANCE STUDY OF SCRAPED SURFACE HEAT EXCHANGER WITH HELICAL RIBBONS" World Academy of Science, Engineering and Technology International Journal of Mechanical, Aerospace, Industrial, Mechatronic and Manufacturing Engineering Vol:10, No:12, 2016
- [10] Eric Dumont, Francine Fayolle, Jack Legrand, "FLOW REGIMES AND WALL SHEAR RATES DETERMINATION WITHIN SCRAPED SURFACE HEAT EXCHANGER". Journal of Food Engineering, 45, 195-207 (2000).
- [11] Giorgio Pagliarini; Fabio Bozzoli; Sara Rainieri "EXPERIMENTAL INVESTIGATION ON THE HEAT TRANSFER PERFORMANCE OF A SCRAPED SURFACE HEAT EXCHANGER FOR HIGHLY VISCOUS FOODS" Marco Mordacci; Proc. ASME. 49392; 2010 14th International Heat Transfer Conference, Volume 4:713-718. January 01, 2010.
- [12] Jerome Mabit a, Rachida Belhamri a, Francine Fayolle, Jack Legrand, "DEVELOPMENT OF A TIME TEMPERATURE INTEGRATOR FOR QUANTIFICATION OF THERMAL TREATMENT IN SCRAPED SURFACE HEAT EXCHANGERS", Journal of Innovative Food Science and Emerging Technologies, 9, 516-526 (2008).
- [13] Yataghene M, Fayolle F, Legrand J. "CFD ANALYSIS OF THE FLOW PATTERN AND LOCAL SHEAR RATE IN A SCRAPED SURFACE HEAT EXCHANGER". Chem Eng. Process 2008; 47:1550-61.